Science of the Total Environment 894 (2023) 164965

Contents lists available at ScienceDirect

Science of the Total Environment

journal homepage: www.elsevier.com/locate/scitotenv

Application of airborne geophysical survey data in a logistic regression model to improve the predictive power of geogenic radon maps. A case study in Castleisland, County Kerry, Ireland

Mirela Dardac [a], Javier Elío [b], Mirsina M. Aghdam [a], Méabh Banríon [a], Quentin Crowley [a,*]

[a] Geology, School of Natural Sciences, Trinity College Dublin, Ireland
[b] Western Norway University of Applied Sciences, Bergen, Norway

HIGHLIGHTS

- New logistic regression technique improves accuracy and resolution of local geogenic radon maps.
- Predicting indoor radon concentrations using geogenic and geophysical data is effective.
- Equivalent uranium (EqU) and soil permeability are the most significant explanatory variables.
- The model has improved accuracy for the local region, when compared with national indoor radon maps.

GRAPHICAL ABSTRACT

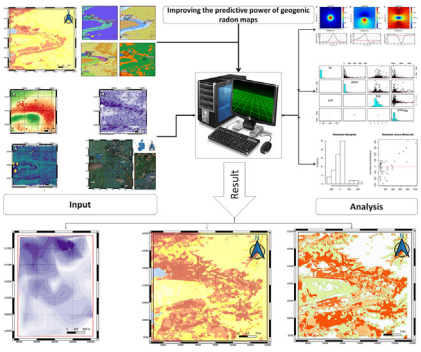

ARTICLE INFO

Editor: Jay Gan

Keywords:
Airborne geophysical survey
Geological variables
Logistic model
Indoor and soil gas radon
Risk map

ABSTRACT

In this study, a novel methodology was investigated to improve the spatial resolution and predictive power of geogenic radon maps. The data inputs comprise indoor radon measurements and seven geogenic factors including geological data (i.e. bedrock and Quaternary geology, aquifer type and soil permeability) and airborne geophysical parameters (i.e. magnetic field strength, gamma-ray radiation and electromagnetic resistivity). The methodology was tested in Castleisland southwest Ireland, a radon-prone area identified based on the results of previous indoor radon surveys. The developed model was capable of justifying almost 75 % of the variation in geogenic radon potential. It was found that the attributes with the greatest statistical significance were equivalent uranium content (EqU) and soil permeability. A new radon potential map was produced at a higher spatial resolution compared with the original map, which did not include geophysical parameter data. In the final step, the activity of radon in soil gas was measured at 87 sites, and the correlation between the observed soil gas radon and geophysical properties was evaluated. The results indicate that any model using only geophysical data cannot accurately predict soil radon activity and that geological information should be integrated to achieve a successful prediction model. Furthermore, we found that EqU is a better indicator for predicting indoor radon potential than the measured soil radon concentrations.

1. Introduction

Radon (^{222}Rn), a colourless radioactive gas, is a decay product of radium (^{226}Ra) which is derived from the radioactive decay of uranium (^{238}U). Radon exposure is associated with an elevated probability of developing lung cancer later in life (Ciotoli et al., 2017). Exposure to higher

* Corresponding author.
E-mail addresses: mdardac@tcd.ie (M. Dardac), mousavim@tcd.ie (M.M. Aghdam), mhughes5@tcd.ie (M. Banríon), crowleyq@tcd.ie (Q. Crowley).

http://dx.doi.org/10.1016/j.scitotenv.2023.164965
Received 7 March 2023; Received in revised form 12 June 2023; Accepted 15 June 2023
Available online 19 June 2023

levels of radon normally occurs indoors (Schmid et al., 2010) and, therefore, to address the adverse health effects of radon exposure it is necessary to identify areas where high indoor radon concentrations are likely to occur. Exposure to indoor radon and its daughter products kills more people in Ireland each year than carbon monoxide poisoning, fires and road accidents combined. It accounts for approximately 13 % of all lung cancer deaths in Ireland (250 annual deaths) (Telecare, 2017). In this regard, the EU Commission developed Council Directive 2013/59/EURATOM, which obligates member states to prepare maps that delineate radon-prone areas in order to protect people from adverse health effects of exposure to ionizing radiation associated with indoor radon. The developed maps are generally on a national scale; however, there is a growing demand for enhanced models which allow better assessment of risk due to exposure to radon by inhabitants at a local-scale.

^{222}Rn gas originates from natural or so-called geogenic sources mainly depending on geology, soil properties, and hydrology (Bossew et al., 2020). Mobilization of radon from source to ground level takes place through three main processes: a) *emanation*, radon atoms formed from the decay of radium escape from the grains (mainly because of recoil) into the interstitial space between the grains; b) *transport*, diffusion and advective flow cause the movement of the emanated radon atoms through the soil profile to the ground surface; and c) *exhalation*, radon atoms that have been transported to the ground surface are then exhaled to the atmosphere (Baskaran, 2016). The presence of joints, faults and fractures, as well as carrier gases like carbon dioxide and methane, facilitate radon transfer to the surface (Lombardi and Voltattorni, 2010). Radon coming from soil and geology under building foundations, which is the major contributor to indoor radon (Al-azmi et al., 2018) (Dentoni et al., 2020) (Aghdam et al., 2021), penetrates the indoor space of buildings through cracks and joints of the foundations (Ciotoli et al., 2017). In addition, building and construction materials, water supply, and natural gasses can all be considered secondary sources of radon in buildings (Dixon, 2005). Ventilation rates, building design, meteorological parameters, and living habits (so-called anthropogenic factors) are other parameters that can significantly affect the concentration of indoor radon (Bossew and Lettner, 2007).

A Geogenic Radon Potential (GRP) map is a promising tool that gives the first evaluation of the amount of radon gas delivered from the geogenic source to ground level (Gruber et al., 2013; Aghdam et al., 2022). The main advantage of a GRP map is that it is independent of anthropogenic factors, and can be produced from existing datasets without site-specific ground-based measurements (Elío et al., 2017). The data (both qualitative and quantitative - see Table 1) that can be used to produce a geogenic radon map may be categorized into two groups, a) parameters related to radon source and b) factors that are indicators of radon mobility and transportation from the source to ground level (Ciotoli et al., 2017; Ielsch et al., 2010) (Scheib et al., 2009) (Omori et al., 2009).

Recently, multivariate regression techniques (e.g., ordinary least square regression, logistic regression, and geographically weighted regression) were used by researchers to estimate geogenic radon potential (Ciotoli et al., 2017; Bossew et al., 2020; Aghdam et al., 2022; Elío et al., 2017). Using such methods, accurate predictions of GRP can be made by using a spatial regression in which a target value (either soil-gas radon or indoor radon activity concentrations) is considered as the response variable, and several proxy variables derived from geological, topographic and geochemical data (Table 1) are set as the explanatory input parameters. According to the geogenic radon risk map of Ireland developed by (Elío et al., 2017), a combination of indoor radon measurements and relevant geological information (i.e. bedrock geology, Quaternary geology, soil permeability and aquifer type) was utilized to develop a radon potential map. Logistic regression was used to predict the probability of having an indoor radon concentration above the national reference level of 200 Bq m^{-3}. The map produced is a good predictor of radon potential on the national scale, however, a more accurate and high-resolution map will allow a better focus of resources on mitigation and improve the effectiveness of planning legislation. This study aims to rebuild the geogenic radon map produced by (Elío et al., 2017) for a radon priority area where one of the highest indoor radon concentrations (49,000 Bq m^{-3}) in Europe has been previously measured (Organo and O'sullivan, 2006). A methodology similar to that study (Elío et al., 2017) was adopted here, however, data from the Tellus airborne geophysical survey (i.e. radiometric, electromagnetic and magnetic) were also included in the prediction model to develop an improved version of the geogenic radon map. The final goal of this study was to achieve a better view of the spatial distribution and levels of risk due to radon exposure and to highlight geographic areas where further measurements or remediation actions could be implemented to reduce the radon-related dose absorbed by inhabitants.

1.1. Geological setting and description of the study area

The study area (Fig. 1) is located in County Kerry in southwest Ireland. It includes three towns; Tralee, Killorglin and Castleisland. The Radon risk map of the Environmental Protection Agency of Ireland (EPA) identifies Castleisland as a Medium-High risk area (E. P. A. (EPA), n.d.). Between 5 and 20 % of homes tested within a 10 km grid registered a radon level above 200 Bq m^{-3}. The recent high-resolution risk map reports a similar risk level (Fig. 1) with some isolated very high-risk spots (30 % chance of higher than reference level indoor radon) (Elío et al., 2017).

The survey area is underlain by Devonian sandstones with subsidiary siltstones and conglomerates, Lower Carboniferous limestones, and middle Carboniferous (Namurian) shales and sandstones folded in *E*-W trending anticlinal-synclinal structures (supplementary file, Appendix A, Fig. A-I-b. The Quaternary deposits in the region of Castleisland mainly consist of glacial till derived from Carboniferous limestones, Namurian shales and sandstones and Devonian sandstones. The limestone is highly karstified with a large network of caves (e.g. Crag cave) and chambers beneath the surface providing a route for dissolved radon to travel (Organo et al., 2004; Appleton et al., 2011). Permeability is generally low for most of the areas however there are areas with medium permeability which correspond to the highest radon risk where they overlap limestone karst (Fig. A-I-d).

Table 1
Examples of data used for geogenic radon mapping, as indicators of radon source and radon mobility (Ciotoli et al., 2017; Aghdam et al., 2021; Gruber et al., 2013; Aghdam et al., 2022; Elío et al., 2017; Ielsch et al., 2010; Scheib et al., 2009; Omori et al., 2009; Li et al., 2023; Zheng et al., 2023; Rääf et al., 2023; Aghdam, 2021; Aghdam et al., 2019).

	Data sets	Description
Radon source Indicators	Soil Gas Radon	Including in-situ and laboratory measurement data on radon and thoron levels
	Geochemical data	e.g., soil and stream sediment K_2O, U, Th, Zr, Y, CaO, SiO_2, Al_2O_3, MgO, and Fe_2O_3 concentrations
	Airborne radiometric	i.e., EqU, EqTh, K, and total gamma counts.
	Gamma spectrometry	Radioelement activity concentrations obtained from in-situ and laboratory tests
	Ambient gamma dose rate	e.g., data obtained from SSNTD LR-115 detectors
	Geology/lithology/soil type	Sometimes regrouped based on indoor radon concentrations
	Other	Altitude, Electromagnetic Field, Magnetic Anomaly, etc.
Radon mobility indicators	Porosity and permeability	Can be measured directly or estimated in a categorical form (i.e., low to high).
	Faults	In the form of calculated fault density, applying a buffer around the fault and measuring the distance from the fault.
	Secondary permeability	Karst features, underground mines (shafts, galleries), caves, main mineral, and thermal groundwater sources
	Carrier gas concentrations	e.g., CO_2, CH_4, etc.

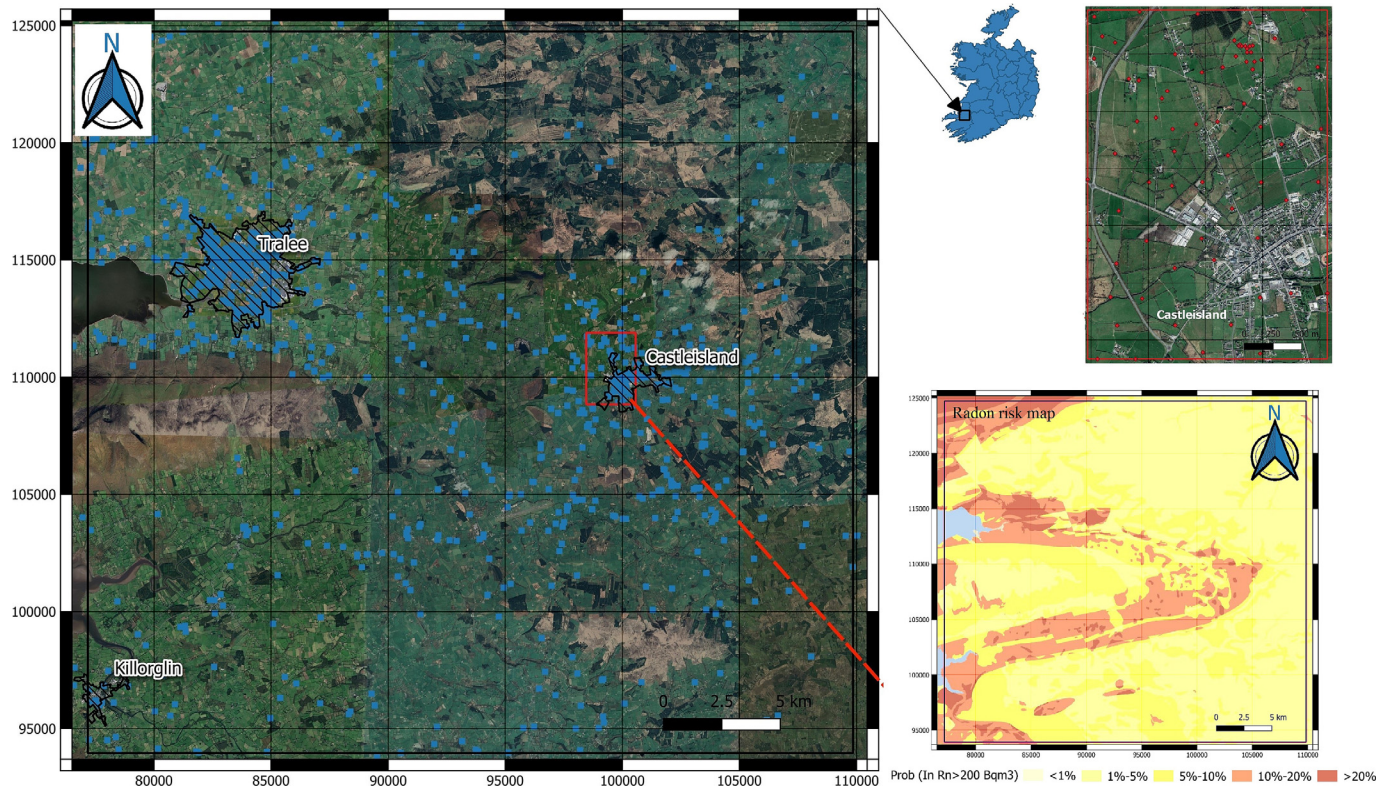

Fig. 1. Satellite map of the study area together with the local extract from the national radon risk map for the Castleisland-Tralee area (Elío et al., 2017). The blue and red dots indicate the indoor and soil gas radon measurement points, respectively. The red rectangle indicates the boundaries of the soil gas field survey area from (Hughes, 2022; Banríon et al., 2022). The position of indoor radon testing has not been indicated on the map for Castleisland, due to GDPR considerations.

The Quaternary map of the area (Fig. A-I-d) expresses that blanket peat covers much of the higher ground and alluvium, river and glaciofluvial gravel deposits are located in the valleys. Because peat has low permeability and unless drained, remains saturated with water, it is generally associated with very low radon risk. In Ireland, aquifers are classed according to their relative groundwater productivity in terms of well and spring yields (Misstear et al., 2018). According to the map of aquifer types (Fig. A-I-a), the most dominant type is a poorly to moderately productive aquifer as a regionally important aquifer.

2. Material and methods

Geogenic data on bedrock and Quaternary geology, aquifer type and permeability (supplementary file, Appendix A, Fig. A-I), which are available on the website of Geological Survey Ireland (http://www.gsi.ie/), together with indoor radon data provided by the EPA and geophysical data set from the Tellus program (i.e. magnetic field strength, gamma-ray radiation and electromagnetic resistivity (supplementary file, Appendix A, Fig. A-II. Further details on the measurement procedures and protocols are available at (Hodgson and Young, 2016))) were employed to build on prior research (Elío et al., 2017) into mapping the geological risk factors at a national level by investigating and achieving a better understanding of the geophysical parameters that influence regional radon potential. Tellus data were introduced to a set of pre-processing operations to reduce the anomalies and increase the accuracy before starting the main analysis. The principal tools for data analysis were the GIS package (both ArcGIS and QGIS) and the open-source R statistical software. ArcGIS and QGIS were used to perform geostatistical analysis and create maps. R was used to analyse the sample values extracted from ArcGIS. The main objective was to identify a statistically significant correlation between radon levels and other effective factors mentioned above. To evaluate spatial correlations, a new logistic regression model in R software was developed which integrated a comprehensive set of both geological and geophysical variables to predict areas with high radon risk.

2.1. Pre-processing of geophysical predictors

As part of the Tellus 2006 pilot program, Castleisland and two other regions were covered by an aerial survey (Organo and O'sullivan, 2006). Magnetic field strength, gamma-ray radiation and electromagnetic resistivity were measured accordingly (supplementary file, Appendix A, Fig. A-II). The survey plane flew in North-South orientated lines with 200 m spacing. Due to fluctuations in winds, the distance between lines varies from approx. 150 m–250 m. In line with the flight path, magnetic readings were taken every 6 m, radiometric readings every 60 m and electromagnetic readings every 15 m. A set of statistical data processing was introduced to the Geophysical data in order to make them suitable for analysis. Details about the data treatment operations conducted on the geophysical data sets can be found in Appendix B (supplementary file).

2.2. Indoor radon data pre-assessment

The available data on the indoor radon concentrations (IRC) survey which was provided by the EPA of Ireland (Fennell et al., 2002) was used in this research. Radon activities were measured by passive alpha track detectors (CR-39), located in homes for a minimum of 3 months and seasonally adjusted to give an annual value. The average outdoor radon concentration (i.e. 5.6 Bq m^{-3}) was subtracted from all the data (Fennell et al., 2002). The average radon concentration of around 12,000 data points was 89 Bq m^{-3}. It is noteworthy to add the population-weighted average of Ireland from a larger dataset (30,000 data points) is around 98 Bq m^{-3} (Elío et al., 2018). 1559 indoor radon readings were available for the study area (Fig. 1 and see Appendix C, Table C–I for summary statistics of these measurements). Given the rural nature of the study area, coverage

is sporadic, however, an experimental variogram was calculated to find out the degree of spatial correlation between the observed IRCs. The variogram of Fig. C–I (Appendix C) which was produced using R software, can justify the high variations in the levels of indoor radon recorded in the neighbouring houses. The level of variance between two samples at zero distance from each other can be explained by a small Sill/Nugget ratio (known as the "nugget effect"). Sill is the level of variance due to the distance between two samples. According to Table C-II, although the range of 2760 m implies that there is a spatial relationship to indoor radon, more than half the potential indoor variance occurs in neighbouring samples. It is noteworthy that 23 % of the available IRCs from the study area exceed the national threshold of 200 Bq m^{-3}.

2.3. Logistic model setting

The logistic regression method is frequently used to evaluate the probability of the occurrence of binary variables; this is achieved by matching the log odds and explanatory variables to a linear model (James et al., 2013). The independent predictor variables can be either continuous (i.e. geophysical data) or categorical (i.e. geogenic factors)

$$\log\left(\frac{P(Y=1|X)}{1-P(Y=1|X)}\right)=\beta_0+\beta_1X_1+\ldots+\beta_nX_n \quad (2)$$

where Y = (0,1) is the binary variable, X = (X_1, …, X_n) are "n" explanatory variables, and β = (β_0, …, β_n) are the regression coefficients to be estimated based on the data. The probability of occurrence is predicted by the logistic function as follows:

$$P(Y=1|X)=\frac{1}{1+e^{-(\beta_0+\beta_1X_1+\ldots+\beta_nX_n)}} \quad (3)$$

In this study, the binary variable (Y) is the indoor radon concentration (equals to 1 if it is higher than the Reference Level (Rn_{Ref}) and 0 if not), modelling the probability of having an indoor radon concentration above the reference level (i.e. 200 Bq m^{-3}) given the explanatory variables (e.g. $n = 7$; aquifer type, permeability, bedrock and Quaternary geology as well as magnetic field intensity, equivalent uranium content and electromagnetic resistivity). Using the glm package in R, with binomial logistic regression options, three models were produced. The first model was the null model, using only the Rn_{Ref} value (i.e. a value of 1 if the indoor radon level exceeded 200 Bq m^{-3} and 0 otherwise). This model is a horizontal line through the mean. As 23 % of indoor radon readings exceeded the reference level, the mean of Rn_{Ref} is 0.23 – corresponding to the logit (Log Odds) value y-axis intercept of −1.167.

The second model integrates the full set of combined geophysical and geological parameters (seven independent variables) to calculate a new radon risk map for the Castleisland region. The third model used only the four geologic parameters employed to generate the national high-resolution risk map – but was restricted to regional category populations. This model was used as a reference to see whether any difference to the national model is because of the influence of the geophysical parameters or the regionalization of the simpler, geology-only model. For each model, the AIC score and the prediction accuracy were calculated and compared to assess the model efficiency and select the model with the highest success rate for the production of the revised geogenic map.

2.4. In-situ soil gas sampling

A field survey (Hughes, 2022; Banríon et al., 2022) including 87 soil radon (see Table C-II for summary statistics) and permeability measurements was considered to investigate the root cause of extreme indoor radon readings observed near the Castleisland area (Fig. 1) and to assess whether soil data can further improve the model and increase the risk map resolution at a local scale.

The RM-2 manufactured by Radon v.o.s. (www.radon.eu/rm2) was used to measure the radon activity of collected soil gas samples. A 1 m hollow tube, with a 'lost tip' attached to the bottom, was hammered vertically into the soil, and the tip was ejected at 80 cm to permit the extraction of a soil-gas sample. Soil-gas permeability was measured by the RADON-JOK device which uses negative pressure created by the pull of a known weight on a diaphragm of known volume to draw air through a probe of a known aperture inserted into the soil. Thus soil-gas flow and thus the gas permeability is calculated from the time taken to fill the volume and using Darcy's equation as follows:

$$Q=F.\left(\frac{k}{\mu}\right).\Delta p \quad ((4)$$

$$k=\frac{Q.\mu}{F.\Delta p} \quad (5)$$

Where Q is the flow rate ($m^3\ s^{-1}$), F is the shape factor (0.159 m for RADON-JOK), k is the permeability (m^2), μ is the dynamic viscosity of air (1.75×10^{-5} Pa s @ 10C°) and Δp is the pressure difference (Pa). Q is calculated from the time taken to fill the 2 l volume of the diaphragm. The pressure is provided by one of three possible options; no weight, one or two weights, applying the pressure values of 0, 2160 or 3750 Pa, respectively. The geo-referenced recorded values of soil gas radon were imported into QGIS and using the Kriging tool, and a spatial distribution of soil gas radon was obtained (Fig. C-II, Appendix C).

3. Results

3.1. Grouping indoor radon data according to geogenic variables and geophysical relationships

Table 2 shows the results of a regression analysis which represents the attributed risk scores of the study area, as well as the categories of geological parameters classified with respect to the percentage of indoor radon data that exceed the national reference level of 200 Bq m^{-3}. According to this table, the percentages of observed IRCs exceeding the reference level increase for the higher predicted risk ranges. The highest percentage of exceeding IRCs (29.8 %) amongst different bedrock geologies was found in Visean limestone and calcareous shale. Differences in the percentage of exceeding IRCs for various types of Quaternary geology are distinct. This finding is significant in that it means that Quaternary geology may be utilized to distinguish between the radon behaviours of different deposits. Both aquifer type and permeability classes were also found to be useful for differentiating radon properties. The highest percentages of exceeding radon values were observed in the karst features (29.8 %) and the units with medium permeability (33.2 %) Note that for the high permeability class, the number of indoor radon data was not sufficient for analysis. The reason for the occurrence of elevated IRCs in these two parameters is related to the presence of factors that facilitate radon mobility in these features. In general, the geology (representative of radon source) together with permeability (as an indicator of radon mobility) were found to be the most important contributors to the occurrence of exceeded levels of indoor radon concentrations. A full discussion of the relationship between radon soil gas and indoor radon for this specific study area can be found in (Banríon et al., 2022).

Fig. 2 displays a Pearson's correlation matrix for indoor radon and geophysical data. The diagonal axis shows the histogram of each property. The top right half of the matrix plots each combination of the parameters with a red trend line. The bottom left half of the matrix computes the Pearson correlation coefficient (PCC), with the text size scaled by value. As shown in this figure, a PCC value of 0.27, indicates a weak and positive correlation between indoor radon and equivalent uranium content. This is because indoor radon is a complex function of various geogenic and anthropogenic factors and therefore none of the geophysical parameters alone can be representative of the indoor radon activity. A model that includes effective parameters, including geological factors, as much as possible would be preferred.

Table 2
Categories of geological parameters classified with respect to the % of indoor radon that exceeded the reference level - Groups highlighted in grey had an insufficient number of samples and were excluded from the regression analysis.

	Site Risk Rating				
	Very High	High	Medium	Low	Total
$N \geq 200$ Bq m^{-3}	153	129	62	22	366
$N < 200$ Bq m^{-3}	243	305	406	231	1185
Radon > Ref	38.6 %	29.7 %	13.2 %	8.7 %	23.6 %
Prediction	> 20 %	10 % to 20 %	5 % to 10 %	1 % to 5 %	
	Bedrock Group				
	Visean limestone & calcareous shale	Tournaisian limestone	Namurian shale, sandstone, siltstone & coal	Sandstone, conglomerate & mudstone	
$N \geq 200$ Bq m^{-3}	234	85	45	2	
$N < 200$ Bq m^{-3}	551	286	302	46	
Radon > Ref	29.8 %	22.9 %	13.0 %	4.2 %	
Prediction	15.33 %	9.35 %	6.01 %	6.86 %	
	Quaternary Geology				
	Sandstone till	Limestone till	Sandstone and shale till	Peat	Glacio-fluvial
$N \geq 200$ Bq m^{-3}	255	88	21	2	0
$N < 200$ Bq m^{-3}	711	336	108	26	4
Radon > Ref	26.4 %	20.8 %	16.3 %	7.1 %	0.0 %
Prediction	14.92 %	12.32 %	8.62 %	5.54 %	7.35 %
	Aquifer Type				
	Karst	Poorly productive fissured (Moderate)	Poorly productive fissured (Unproductive)	Intergranular	
$N \geq 200$ Bq m^{-3}	260	102	4	0	
$N < 200$ Bq m^{-3}	672	494	18	1	
Radon > Ref	27.9 %	17.1 %	18.2 %	0.0 %	
Prediction	19.32 %	8.27 %	10.03 %	7.11 %	
	Permeability				
	L	M	H		
$N \geq 200$ Bq m^{-3}	65	300	1		
$N < 200$ Bq m^{-3}	569	604	12		
Radon > Ref	10.3 %	33.2 %	7.7 %		
Prediction	13.87 %	14.58 %	6.23 %		

Previous research at the University of Bristol, UK has shown that the presence of high levels of low-frequency electromagnetic fields near high-voltage cables can increase the accumulation of radon particles by up to 18 times (Haider et al., 2018). In order to understand the contribution of different levels of equivalent uranium (EqU), resistivity and magnetic field to the elevated indoor radon levels (i.e. exceeding the reference level), the IRC data were sorted by each category with the number of samples graphed against the number of samples exceeding the reference level (Fig. D–I, Appendix D). Although this display can give a false sense of linearity, it identifies zones of relatively constant slope. According to this figure, there is an almost universal increase in the rate of indoor radon samples exceeding the threshold level with the level of equivalent uranium. This increases from a rate of almost 10 % for low EqU values to over 50 % for the upper quartile of EqU values. The resistivity shows an increasing rate of high radon values with higher resistivity however the rates are relatively uniform – and relatively close to the overall concentration of indoor radon readings (23 %). The rates relative to magnetic field strength are complex, with plateaus at a mid and high level with a low slope – around 10 %.

In Table 3, the percentage of indoor radon values exceeding the reference level of geophysical variables was classified according to the zones identified in Fig. D–I, Appendix D. According to this table, for the resistivity and total magnetic field parameters, it was not possible to distinguish between the per cent of IRCs greater than the reference value. However, the occurrence of exceeded indoor radon activities was found to increase by shifting the equivalent uranium concentration. About 54 % of values >200 Bq m^{-3} were observed where uranium activity exceeded 2.04 ppm. A threshold EqU value of 2.04 ppm could therefore be used as an initial indicator when searching for radon-prone areas, especially given that the estimated average soil U concentration for Ireland is approximately 1 ppm (mg/kg).

3.2. Logistic regression model

Table 4 expresses the AIC score and the prediction accuracy for the three models introduced in Section 2.3. The new regional model has a slightly higher successful prediction rate of 77.9 % compared to the prediction accuracy of the national geology-only model (76.5 %). *Re*-calculating the model using the same factors as the national model (e.g. no geophysical variables) but limiting the calculation to the regional area has a successful prediction rate of 76.2 %, marginally worse than the national model. This could be due to the limited number of samples within some geological categories when restricted to the local region.

Based on these results, the full geogenic model was selected as the best model. The full parameters for this model are listed in Table 5. The attributes with the greatest statistical significance are EqU and soil permeability. These attributes also have the largest coefficients indicating the greatest influence on the predicted indoor radon level.

The intercept value of 257.5 is unusual as this logit value equates effectively to a probability of "1", indicating 100 % odds of exceeding the radon threshold. It has a much greater magnitude than the other coefficients. The reason for this is the very high values of magnetic field strength (approx. 48,000), which with a negative coefficient means that a high magnetic field will act to reduce the overall radon risk. The significance (*P*-value) of this field is also low.

3.3. The revised version of the geogenic radon map and comparison with the national radon map

Using the full geogenic model parameters (Table 5), a new raster map (Fig. 3) was created in ArcGIS which combined the coefficients based on the underlying geological categories and scaled geophysical categories on a 20 m*20 m grid. The values were converted from log-odds (L) back to probability score (P) using the inverse log-odds (Eq. 3).

The new map was validated by calculating a confusion matrix (Table 6), using a model that predicts the likelihood of an outcome (e.g. radon above 200 Bq m^{-3}) and a threshold for making a decision (e.g. if $P > 0.5$, then TRUE). Any change in the threshold of decision alters the ratios of the confusion matrix. Based on this, the Receiver Operating Curves (ROC) of the

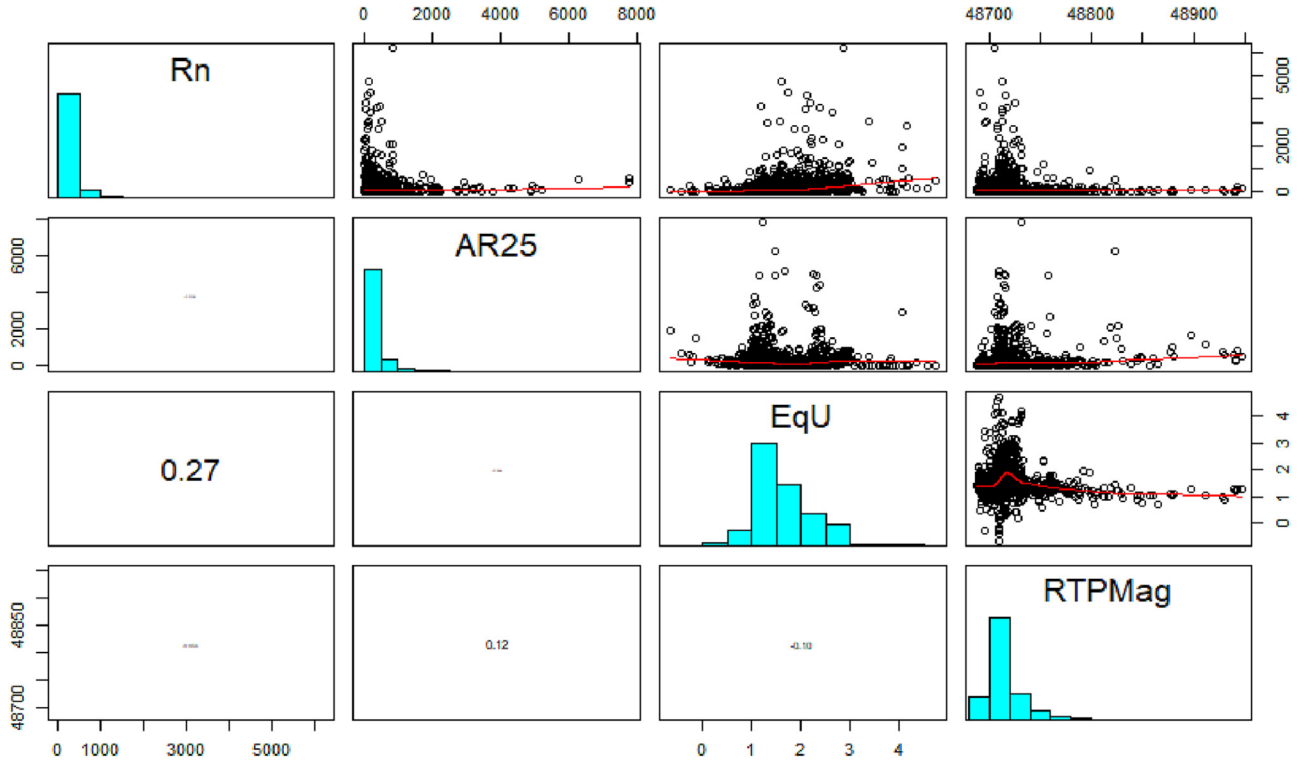

Fig. 2. Pearson correlation matrix of Indoor Radon (Rn) and geophysical attributes (AR25 – Resistivity @ 25Khz, EqU – equivalent uranium and RTPMag, corrected magnetic field strength).

new regional model and the original national indoor radon risk model were plotted (Fig. 13). The area under the curve (AUC) of the two graphs is 0.77 for the regional full geogenic map and 0.68 for the national risk map, indicating that the new regional model improves the national risk map in the area.

The new regional map shows a significant improvement in risk prediction compared to the national risk map. Using the QGIS and the Raster calculator tool, the percentages of difference between new risks scores (Fig. 3-left) and the risk levels from the national radon map (Fig. 1) for different areas of the study were calculated in Fig. 3- right. According to this figure, less than a 15 % difference is predicted for most of the areas and the maximum difference range is about 34–38 %.

Table 3
% of IRCs exceeding 200 Bq m^{-3} within each group of constant slope for geophysical attributes. Groups refer to regions divided by green bars in Fig. D–I, Appendix D, considering an increasing group order from left to right.

Group	0	1	2	3
	Resistivity (Ω.m)			
Lower limit	–	92	168	407
Upper limit	92	168	407	–
N ≥ 200 Bq m^{-3}	84	61	118	103
N < 200 Bq m^{-3}	352	297	281	255
Radon > Ref	19.3 %	17.0 %	29.6 %	28.8 %
	Equivalent uranium concentration (ppm)			
Lower limit	–	1.2	1.59	2.04
Upper limit	1.2	1.59	2.04	–
N ≥ 200 Bq m^{-3}	34	70	73	189
N < 200 Bq m^{-3}	308	448	263	166
Radon > Ref	9.9 %	13.5 %	21.7 %	53.2 %
	Total magnetic field strength (nT)			
Lower limit	–	48,697	48,707	48,728
Upper limit	48,697	48,707	48,728	–
N ≥ 200 Bq m^{-3}	34	28	275	29
N < 200 Bq m^{-3}	116	250	572	247
Radon > Ref	22.7 %	10.1 %	32.5 %	10.5 %

3.4. Correlation of soil radon and geophysical properties

As shown in Fig. 4, all possible pair combinations of the soil radon reading, the apparent resistivity @ 25 kHz (AR25), equivalent uranium (EqU) and total magnetic field strength after RTP correction (RTPMag) were evaluated using a Pearson's correlation matrix. There is a significant (p-value <0.05) correlation between the measured soil radon value and the EqU and an inverse correlation to the RTPMag value. The correlation is weaker between soil radon and AR25 but still statistically significant ($P = 0.026$). It can be understood that high soil radon values are concentrated in areas with lower resistivity readings however, there are insufficient samples in high-resistivity areas to draw a strong conclusion (for additional information see the supplementary file Fig. D-II and Fig. A-II. There is also a moderate positive correlation (0.57) between resistivity and magnetic field. The correlation coefficient between indoor and soil radon was 0.41, indicating a moderate positive correlation, though statistically significant with a p-value of the order of 10^{-5}. This is a weaker relationship than might be expected and suggests that EqU is more important in predicting indoor radon than a measured soil radon value.

There are insufficient samples in the different geological categories to break down the in-situ samples and attempt logistic regression including geological information. Instead, linear models were calculated using

Table 4
Summary of results for model selection.

Model	AIC	Prediction accuracy
Null Model	1687.6	50 %
Full, Regional Geogenic Model	1443.4	77.9 %
Regional Geology Only Model	1531.2	76.2 %
National Geology Only Model	–	76.5 %

Table 5
Model parameters of the recalculated logistic regression model incorporating Geogenic (Bedrock geology, Quaternary geology, Aquifer type and Permeability) and Geophysical data (Resistivity @ 25 KHz, RTP corrected magnetic field strength and equivalent uranium).

Coefficient	Parameter		Estimate	Std. Error	z value	Pr(>|z|)
β0	(Intercept)		257.5	170.5	1.511	0.1309
β1	AR25		0.0001912	0.0000958	1.996	0.0459*
β2	EqU		1.179	0.1349	8.735	<2e-16***
β3	RTPMag		−0.005389	0.003498	−1.541	0.1234
β4	Bedrock geology	ORS, sandstone, conglomerate & mudstone	0	–	–	–
		Namurian shale, sandstone, siltstone & coal	0.3752	0.8139	0.461	0.6448
		Tournaisian limestone	1.797	0.8003	2.246	0.0247*
		Visean limestone & calcareous shale	1.05	0.8112	1.295	0.1955
β5	Aquifer type	Poorly productive fissured (Unproductive)	0	–	–	–
		Poorly productive fissured (Moderate)	0.7744	0.6502	1.191	0.2336
		Karst	0.3518	0.6735	0.522	0.6014
β6	Permeability class	L	0	–	–	–
		M	0.9108	0.1795	5.074	3.90E-07***
β7	Quaternary geology	Peat	0	–	–	–
		Sandstone and shale till	−0.6006	0.8324	−0.722	0.4706
		Limestone till	−0.9059	0.7847	−1.155	0.2483
		Sandstone till	−0.3646	0.7716	−0.473	0.6365

Significance codes: 0 '***' 0.001 '**' 0.01 '*' 0.05 '.' 0.1 ' ' 1.

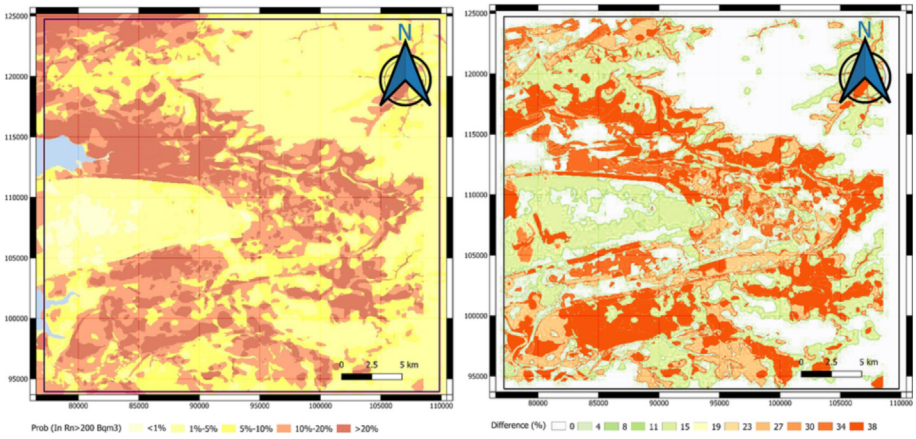

Fig. 3. Revised version of the geogenic radon map for the Castleisland area (left) and Difference plot of new risk score versus national risk score. The map shows the uncertainty of prediction while comparing the new map and the original radon map for the study area (right).

combinations of resistivity, equivalent uranium and magnetic field strength as independent variables. Polynomials up to 3rd order were tested however 3rd order polynomials produced only a marginally better fit compared to 2nd order polynomials (based on Akaike information criterion, AIC) (Eq. 7).

$$Soil\ Radon = \beta_0 + \beta_1 * (Eq.U)^2 + \beta_2 * RTPMag + \beta_3 (RTPMag)^2 \quad (7)$$

Where $\beta_0 = 2.87E+09$, $\beta_1 = 3.24E+01$, $\beta_2 = -1.18E+08$ and $\beta_3 = 1.21E+06$. The fitted polynomial models excluded resistivity as an independent variable.

According to Fig. D-III, the residuals of the model are poor, indicating a poor fit for the data in general. The magnitude of the residuals is the same magnitude as the measured values. Hence, the model using only geophysical data cannot accurately predict soil radon despite the apparent correlation. Therefore, EqU (and perhaps equivalent thorium) survey data could be possible substitutes for geogenic radon (and perhaps thoron) mapping if only combined with relevant geogenic variables (e.g. geology).

Table 6
Sample confusion matrix with a decision at threshold 0.5.

Predicted result	Actual result	
	Radon ≥200 Bq m^{-3}	Radon <200 Bq m^{-3}
Radon ≥ 200 Bq m^{-3}	True positive - 142	False positive - 98
Radon <200 Bq m^{-3}	False negative - 224	True negative -1093

4. Discussion

As a result of this study, the accuracy and resolution of the national geogenic radon map of Ireland for the Castleisland/Tralee area were improved. This achievement is mainly because of a) the inclusion of additional effective parameters such as airborne geophysical data (in particular EqU) and b) the use of a more detailed scale (i.e. 1:100 K) geological map. For the national radon map development (Elío et al., 2017), a simplified 1:1 M scale bedrock map of Ireland was utilized. Due to this, some important details were lost in the risk analysis. For example, the Clare Shale Formation, which was found to pose a significant risk factor due to its elevated uranium concentration, was merged into the category of Namurian shale, sandstone, siltstone and coal. The area underlain by Clare shale bedrock is restricted to a narrow band with a total area of only 11 km^2 (of the 1000 km^2 investigated). The Quaternary deposits in the area around Tralee are limestone or sandstone-derived till however, likely, glacial action has also eroded the Clare shale bedrock and distributed this shale till in the formation. In addition, the karst structures beneath Castleisland and Tralee may distribute radon generated from uranium/radium-rich lithologies/sediments some distance from the source. The Clare Shale Formation, although spatially restricted in distribution, could have a significant impact on

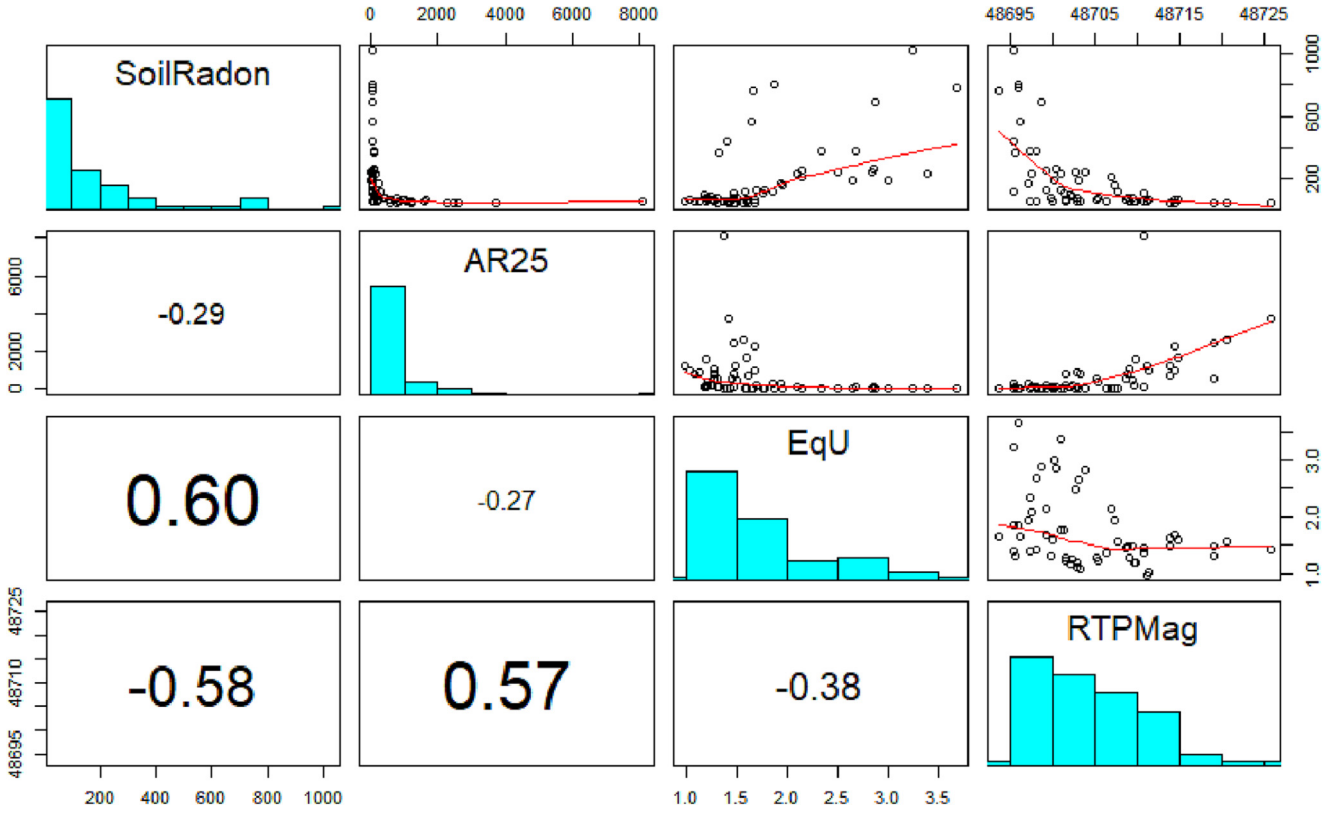

Fig. 4. Comparison of correlation between soil radon and geophysical attributes (AR25 – Resistivity @ 25Khz, EqU – equivalent uranium and RTPMag, corrected magnetic field strength).

regional radon. This can be explained by the unique radon characteristics of shale deposits. Enhanced levels of uranium content (i.e. the parent element of radon) in these formations (especially black and alum shales) make them potential radon emitters (Fennell et al., 2002).

A moderate correlation was found between the observed indoor radon and the measured soil radon activities. By evaluation of the correlations between soil and indoor radon, it was found that the EqU integrated with geological information is a better predictor of indoor radon level compared to soil gas alone. On the other hand, a good correlation was obtained between soil gas radon and EqU. Soil gas radon testing which is known as one of the ideal ways to produce a GRP map (Kropat et al., 2015) is time-consuming and sometimes difficult to perform. Soil gas radon results might also be affected by large uncertainties, due to changing physical conditions such as soil moisture, temperature and pressure gradients (Lucchetti et al., 2019). Therefore, where such data are available, airborne radiometric data can be utilized instead of soil gas radon testing to produce GRP maps. It is noteworthy that one of the main advantages of airborne data provided by the Tellus program is that they are available for free in high spatial resolution (generally tens of meters) for most of the island of Ireland. This can provide the feasibility of high-resolution geogenic radon and thoron mapping on a national scale (e.g. (Aghdam et al., 2021; Elio et al., 2020)).

5. Conclusion

A novel methodology was introduced here to produce a local scale geogenic radon map by integrating both geogenic information and airborne geophysical data in a logistic regression model in which indoor radon concentrations were set as the response parameter. The final model has improved the accuracy of national indoor radon maps (Elío et al., 2017; Agency, 2020). The equivalent uranium content (EqU) and soil permeability were found to be the most significant explanatory variables of the prediction model. It was also found that geological parameters should be considered while the production of any geogenic radon model to achieve more realistic predictions. Areas with high permeability (e.g. limestone karst bedrock) and areas underlain by shale formations, in particular the Clare shale, were found to be radon-prone areas (RPA). Most of the anomalies in indoor radon activities correspond with the "EqU" hotspot areas. A band of shale running through the study area, although spatially and stratigraphically limited in extent, was identified as a possible source of enhanced radon concentrations in the area.

The inclusion of resistivity and magnetic data resulted in a small improvement in the model accuracy while increasing its complexity. There appeared to be a net benefit to including these parameters when producing geogenic radon maps but their value in this regard needs further assessment. As an important result of this study, the EqU incorporated with geological information was found to be a promising tool to predict the geogenic radon potential of the Castleisland/Tralee area. This methodology can be efficiently expanded to produce an improved version of the national geogenic radon (or thoron) potential map of Ireland. The methodology described here could be applied to other countries, where such datasets are available, as an effective way of producing geogenic radon maps.

Credit author statement

Mirela Dardac: Investigation, Writing- original draft preparation, Methodology, **Javier Elío:** Supervision and Software validation, **Mirsina M. Aghdam:** Conceptualization, Writing- original draft preparation, Methodology, Visualization, **Meabh Banrion:** Data collection, **Quentin Crowley:** Writing- review and editing, Supervision, Project administration, Funding acquisition.

Data availability

No data was used for the research described in the article.

Declaration of competing interest

The authors declare that they have no conflict of interest.

Acknowledgement

We would like to thank the Environmental Protection Agency (EPA) of Ireland for providing the requested indoor radon readings used in this study. We would like to also appreciate Geological Survey Ireland for giving us access to their datasets. Finally, Mr. George Reynolds commented on an earlier version of the manuscript and helped us to improve the quality of the paper. This research paper interoperates the results and main findings of an MSc degree (Mirela Dardac) and a PhD degree (Méabh Banríon) thesis work from Trinity College Dublin. This work was supported by a SUSI grant to Méabh Banríon.

Appendix A. Supplementary data

Supplementary data to this article can be found online at https://doi.org/10.1016/j.scitotenv.2023.164965.

References

M. M.Aghdam, Modelling of geogenic radon in Sardinia and health risk assessment, Università degli Studi di Cagliari, 2021.

Aghdam, M.M., et al., 2019. Measurements of indoor radon levels and gamma dose rates. Proceedings of the World Congress on New Technologies 0. https://doi.org/10.11159/icepr19.149.

M. M. Aghdam *et al.*, "A study of natural radioactivity levels and radon/thoron release potential of bedrock and soil in Southeastern Ireland," Int. J. Environ. Res. Public Health, vol. 18, no. 5, p. 2709, Mar. 2021, doi: https://doi.org/10.3390/ijerph18052709.

Aghdam, M.M., Dentoni, V., Da Pelo, S., Crowley, Q., 2022. Detailed geogenic radon potential mapping using geospatial analysis of multiple geo-variables—a case study from a high-risk area in SE Ireland. Int. J. Environ. Res. Public Health 19 (23), 15910. https://doi.org/10.3390/IJERPH192315910.

Al-azmi, D., Okeyode, I.C., Alatise, O.O., Mustapha, A.O., 2018. Setup and procedure for routine measurements of radon exhalation rates of building materials. Radiat. Meas. 112 (January), 6–10. https://doi.org/10.1016/j.radmeas.2018.03.001.

J. D. Appleton, E. Doyle, D. Fenton, and C. Organo, Radon potential mapping of the Tralee–Castle Island and Cavan areas (Ireland) based on airborne gamma-ray spectrometry and geology, J. Radiol. Prot., vol. 31, no. 2, p. 221, May 2011, doi: https://doi.org/10.1088/0952-4746/31/2/002.

Banríon, M.H., Elío, J., Crowley, Q.G., 2022. Using geogenic radon potential to assess radon priority area designation, a case study around Castleisland, Co. Kerry, Ireland. J. Environ. Radioact. 251–252, 106956. https://doi.org/10.1016/j.jenvrad.2022.106956.

Baskaran, M., 2016. Radon: A Tracer for Geological. Springer International Publishing, Geophysical and Geochemical Studies.

Bossew, P., Lettner, H., 2007. Investigations on indoor radon in Austria, Part 1: seasonality of indoor radon concentration. J. Environ. Radioact. 98 (3), 329–345. https://doi.org/10.1016/j.jenvrad.2007.06.006.

P. Bossew *et al.*, "Development of a geogenic radon hazard index—concept, history, experiences," Int. J. Environ. Res. Public Health, vol. 17, no. 11, p. 4134, Jun. 2020, doi: https://doi.org/10.3390/ijerph17114134.

G. Ciotoli *et al.*, "Geographically weighted regression and geostatistical techniques to construct the geogenic radon potential map of the Lazio region: a methodological proposal for the European Atlas of Natural Radiation," J. Environ. Radioact., vol. 166, pp. 355–375, Jan. 2017, doi: https://doi.org/10.1016/J.JENVRAD.2016.05.010.

V. Dentoni *et al.*, "Natural radioactivity and radon exhalation rate of Sardinian dimension stones," Constr. Build. Mater., vol. 247, p. 118377, Jun. 2020, doi: https://doi.org/10.1016/j.conbuildmat.2020.118377.

Dixon, D., 2005. Understanding radon sources and mitigation in buildings. J. Build. Apprais. 1 (2), 164–176.

E. P. A. (EPA), 2002. Radon in Dwellings: The National Radon Survey. *Environmental Protection Agency (EPA)*, Environmental Protection Agency (EPA).

J. Elío, Q. Crowley, R. Scanlon, J. Hodgson, and S. Long, "Logistic regression model for detecting radon prone areas in Ireland," Sci. Total Environ., vol. 599–600, pp. 1317–1329, Dec. 2017, doi: https://doi.org/10.1016/J.SCITOTENV.2017.05.071.

Elio, J., et al., 2020. Application of airborne radiometric surveys for large-scale geogenic radon potential classification. J. Eur. Radon Assoc. 1.

Elío, J., Crowley, Q., Scanlon, R., Hodgson, J., Zgaga, L., 2018. Estimation of residential radon exposure and definition of radon priority areas based on expected lung cancer incidence. Environ. Int. 114, 69–76. https://doi.org/10.1016/j.envint.2018.02.025.

Environmental Protection Agency (EPA), EPA Maps, 2020. [Online]. Available: https://gis.epa.ie/EPAMaps/Radon?easting=?&northing=?&lid=EPA:RAD_RadonMap. [Accessed: 20-May-2021].

Fennell, S.G., et al., 2002. Radon in Dwellings: The Irish National Radon Survey. Radiological Protection Institute of Ireland Dublin.

V. Gruber, P. Bossew, M. De Cort, and T. Tollefsen, "The European map of the geogenic radon potential," J. Radiol. Prot., vol. 33, no. 1, pp. 51–60, Jan. 2013, doi: https://doi.org/10.1088/0952-4746/33/1/51.

Haider, L.M., Shareef, N.R., Darwoysh, H.H., Mansour, H.L., 2018. Study of the effect of electromagnetic fields on indoor and outdoor radon concentrations. J. Phys. Conf. Ser. 1003 (1), 12104.

Hodgson, J., Young, M., 2016. 2. The Tellus airborne geophysical surveys and results, *Unearthed impacts Tellus Surv. north Ireland*. Dublin. R. Irish Acad. https://doi.org/10.3318/978-1-908996-88-6.ch2.

Hughes, M.B., Elio, J., Crowley, Q.G., 2022. A user's guide to radon priority areas, examples from Ireland. J. Eur. Radon Assoc. 3.

G. Ielsch, M. E. Cushing, P. Combes, and M. Cuney, "Mapping of the geogenic radon potential in France to improve radon risk management: methodology and first application to region Bourgogne," J. Environ. Radioact., vol. 101, no. 10, pp. 813–820, Oct. 2010, doi: https://doi.org/10.1016/j.jenvrad.2010.04.006.

James, G., Witten, D., Hastie, T., Tibshirani, R., 2013. An Introduction to Statistical Learning. vol. 112. Springer.

G. Kropat *et al.*, "Improved predictive mapping of indoor radon concentrations using ensemble regression trees based on automatic clustering of geological units," J. Environ. Radioact., vol. 147, pp. 51–62, Sep. 2015, doi: https://doi.org/10.1016/j.jenvrad.2015.05.006.

Li, P., Sun, Q., Geng, J., Jing, X., Tang, L., 2023. Study on the characteristics of radon exhalation from rocks in coal fire area based on the evolution of pore structure. Sci. Total Environ. 862, 160865. https://doi.org/10.1016/j.scitotenv.2022.160865.

Lombardi, S., Voltattorni, N., 2010. Rn, He and CO2 soil gas geochemistry for the study of active and inactive faults. Appl. Geochem. 25 (8), 1206–1220. https://doi.org/10.1016/j.apgeochem.2010.05.006.

C. Lucchetti *et al.*, "Integrating radon and thoron flux data with gamma radiation mapping in radon-prone areas. The case of volcanic outcrops in a highly-urbanized city (Roma, Italy)," *J. Environ. Radioact.*, vol. 202, no. September 2018, pp. 41–50, 2019, doi: https://doi.org/10.1016/j.jenvrad.2019.02.004.

Misstear, B., Gill, L., McKenna, C., Foley, R., 2018. Hydrology and Communities: A Hydrogeological Study of Irish Holy Wells.

Omori, Y., et al., 2009. Preseismic alteration of atmospheric electrical conditions due to anomalous radon emanation. Phys. Chem. Earth, Parts A/B/C 34 (6), 435–440. https://doi.org/10.1016/j.pce.2008.08.001.

Organo, C., O'sullivan, F., 2006. The Castleisland Radon Survey (Sw Ireland).

C. Organo *et al.*, High radon concentrations in a house near Castleisland, County Kerry (Ireland)–identification, remediation and post-remediation, J. Radiol. Prot. Off. J. Soc. Radiol. Prot., vol. 24, no. 2, pp. 107–120, Jun. 2004, doi: https://doi.org/10.1088/0952-4746/24/2/001.

Rääf, C.L., Tondel, M., Isaksson, M., Wålinder, R., 2023. Average uranium bedrock concentration in Swedish municipalities predicts male lung cancer incidence rate when adjusted for smoking prevalence: indication of a cumulative radon induced detriment. Sci. Total Environ. 855, 158899. https://doi.org/10.1016/j.scitotenv.2022.158899.

C. Scheib, J. D. Appleton, J. C. H. Miles, B. M. R. Green, T. S. Barlow, and D. G. Jones, "Geological controls on radon potential in Scotland," Scott. J. Geol., vol. 45, no. 2, pp. 147–160, Nov. 2009, doi: https://doi.org/10.1144/0036-9276/01-401.

K. Schmid, T. Kuwert, and H. Drexler, "Radon in indoor spaces: an underestimated risk factor for lung cancer in environmental medicine," Dtsch. Arztebl. Int., vol. 107, no. 11, pp. 181–186, Mar. 2010, doi: https://doi.org/10.3238/arztebl.2010.0181.

Telecare, Radon exposed the gas that kills 250 each year in Ireland, 2017.

Zheng, X., Sun, Q., Jing, X., Yang, D., Jia, H., 2023. Evolution of pore structure and radon exhalation characterization of porous media grouting. Sci. Total Environ. 865, 161352. https://doi.org/10.1016/j.scitotenv.2022.161352.